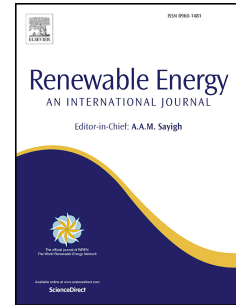


# Accepted Manuscript

Evolutionary computation for wind farm layout optimization

Dennis Wilson, Silvio Rodrigues, Carlos Segura, Ilya Loshchilov, Frank Hutter, Guillermo López Buenfil, Ahmed Kheiri, Ed Keedwell, Mario Ocampo-Pineda, Ender Özcan, Sergio Ivvan Valdez Peña, Brian Goldman, Salvador Botello Rionda, Arturo Hernández-Aguirre, Kalyan Veeramachaneni, Sylvain Cussat-Blanc



PII: S0960-1481(18)30363-X

DOI: [10.1016/j.renene.2018.03.052](https://doi.org/10.1016/j.renene.2018.03.052)

Reference: RENE 9921

To appear in: *Renewable Energy*

Received Date: 15 July 2017

Revised Date: 7 March 2018

Accepted Date: 20 March 2018

Please cite this article as: Wilson D, Rodrigues S, Segura C, Loshchilov I, Hutter F, Buenfil GuillermoLó, Kheiri A, Keedwell E, Ocampo-Pineda M, Özcan E, Peña SIV, Goldman B, Rionda SB, Hernández-Aguirre A, Veeramachaneni K, Cussat-Blanc S, Evolutionary computation for wind farm layout optimization, *Renewable Energy* (2018), doi: 10.1016/j.renene.2018.03.052.

This is a PDF file of an unedited manuscript that has been accepted for publication. As a service to our customers we are providing this early version of the manuscript. The manuscript will undergo copyediting, typesetting, and review of the resulting proof before it is published in its final form. Please note that during the production process errors may be discovered which could affect the content, and all legal disclaimers that apply to the journal pertain.

# Evolutionary computation for wind farm layout optimization

Dennis Wilson<sup>a</sup>, Silvio Rodrigues<sup>b</sup>, Carlos Segura<sup>d</sup>, Ilya Loshchilov<sup>e</sup>,  
 Frank Hutter<sup>e</sup>, Guillermo López Buenfil<sup>d</sup>, Ahmed Kheiri<sup>f</sup>, Ed Keedwell<sup>g</sup>,  
 Mario Ocampo-Pineda<sup>d</sup>, Ender Özcan<sup>h</sup>, Sergio Ivvan Valdez Peña<sup>d</sup>,  
 Brian Goldman<sup>i</sup>, Salvador Botello Rionda<sup>d</sup>, Arturo Hernández-Aguirre<sup>d</sup>,  
 Kalyan Veeramachaneni<sup>c</sup>, Sylvain Cussat-Blanc<sup>a</sup>

<sup>a</sup> *University of Toulouse - IRIT - CNRS UMR5505,*  
 {dennis.wilson, sylvain.cussat-blanc}@irit.fr

<sup>b</sup> *Delft University of Technology, s.m.fragosorodrigues@tudelft.nl*

<sup>c</sup> *MIT - LIDS, kalyanv@mit.edu*

<sup>d</sup> *Center for Research in Mathematics,*  
 {carlos.segura, manuel.lopez, mario.ocampo, ivvan, botello, artha}@cimat.mx

<sup>e</sup> *University of Freiburg, {ilya, fh}@cs.uni-freiburg.de*

<sup>f</sup> *Lancaster University, a.kheiri@lancaster.ac.uk*

<sup>g</sup> *University of Exeter, e.c.keedwell@exeter.ac.uk*

<sup>h</sup> *University of Nottingham, ender.ozcan@nottingham.ac.uk*

<sup>i</sup> *Michigan State University, brianwgoldman@acm.org*

---

## Abstract

This paper presents the results of the second edition of the Wind Farm Layout Optimization Competition, which was held at the 22<sup>nd</sup> Genetic and Evolutionary Computation Conference (GECCO) in 2015. During this competition, competitors were tasked with optimizing the layouts of five generated wind farms based on a simplified cost of energy evaluation function of the wind farm layouts. Online and offline APIs were implemented in C++, Java, Matlab and Python for this competition to offer a common framework for the competitors. The top four approaches out of eight participating teams are presented in this paper and their results are compared. All of the competitors' algorithms use evolutionary computation, the research field of the conference at which the competition was held. Competitors were able to downscale the optimization problem size (number of parameters) by casting the wind farm layout problem as a geometric optimization problem. This strongly reduces the number of evaluations (limited in the scope of this competition) with extremely promising results.

*Keywords:* Wind farm layout optimization, evolutionary algorithm, competition

---

## 1 1. Introduction

2 Wind farm design is a complex task and the recent trend of larger farm  
3 sizes has greatly increased demands on designers. Traditionally, a small, well-  
4 connected, land area is divided into smaller cells and turbine placement among  
5 cells is decided through a simple search algorithm with a pre-specified cost  
6 function. This function is usually limited to minimizing inter-turbine wake  
7 interferences and thus maximizing energy capture. Few approaches consider  
8 additional factors such as operation and maintenance costs, turbine costs, or  
9 cable layout.

10 Modern farms cover large areas and boast hundreds, and sometimes even  
11 thousands, of turbines. The layout design process is iterative, computationally  
12 expensive, burdened with global and local constraints, and ultimately controlled  
13 by subjective assessments due to the involvement of a variety of stakeholders.  
14 During each step, designers must either refine an incremental layout or pro-  
15 pose a new layout which they have generated by incorporating new constraints.  
16 Additionally, evaluating a layout requires varied multi-disciplinary models and  
17 sub-modules that are extremely computationally expensive.

18 The wind farm layout optimization problem is the identification of turbine  
19 positions in a 2-D plane such that the energy capture is maximized while costs  
20 associated with a number of other factors are minimized. The energy capture  
21 for a turbine takes into account the wind scenario (wind force distribution and  
22 terrain), the turbines' power curve (power generated by the turbine in function  
23 of the wind input) and wake effects (inter-turbine interferences) [1].

24 When optimizing both the position and the number of turbines to build,  
25 genetic algorithms (GAs) are commonly used to optimize wind farm layout.  
26 The farm area is discretized with a grid [2, 3, 4, 5, 6, 7, 8]. [The GA optimizes a  
27 binary genome in which each gene represents the presence or absence of a turbine  
28 in each cell of the grid, therefore both optimizing the number of turbines and  
29 their discrete placement.](#) Other techniques have been evaluated using particle  
30 swarm optimization [9, 10, 11] and local modification with different optimization  
31 algorithms [12, 13]. Wilson et al. have also proposed an innovative interactive  
32 approach based on cell-based developmental model in [14]. [Interested readers  
33 can find overviews of existing methods for wind farm layout optimization in  
34 Khan et al. \[15\] and Samorani \[16\].](#)

35 In this paper, we report on a competition we ran at the Genetic and Evo-  
36 lutionary Computation Conference 2015 (GECCO 2015) during which experts  
37 from the evolutionary computation community optimized wind farm layouts.  
38 Eight teams participated and proposed innovative algorithms, all evaluated in  
39 the same context: the same wind scenarios, power curve and wake effect mod-  
40 els. This paper presents the results of the top 4 participants and is organized  
41 as follows. Section 2 presents the rules and the framework used during the  
42 competition. Section 3 details the top 4 algorithms of the competition, which  
43 are then compared with a standard binary GA in section 4. Finally, this article  
44 discusses these algorithms and opens novel questions that could be addressed  
45 using evolutionary algorithms in this domain of research.

## 46 2. Competition rules and framework

### 47 2.1. Competition rules

48 Whereas the first edition of the wind farm layout optimization competition,  
 49 held at the 2014 Genetic and Evolutionary Computation COncference (GECCO),  
 50 consisted in only optimizing the wake free ratio (actual energy output over po-  
 51 tential output without wake), the second edition focuses on the economical  
 52 viability of the produced layouts. Layouts generated by the competitors' al-  
 53 gorithms are evaluated in the cloud on 5 unknown wind scenarios (wind rose,  
 54 layout shape and obstacles, turbine specifications, etc.) using the cost func-  
 55 tion presented below. In order to keep the computation cost acceptable, the  
 56 competitors have a finite number of possible evaluations: they can only call  
 57 the evaluation function 10,000 times for all 5 scenarios combined. This limited  
 58 amount of evaluation credits aims to represent the CPU cost of layout evalua-  
 59 tion and to promote efficient algorithms. This metric was preferred to CPU time  
 60 because the computation was held on a shared research cluster with no exclusive  
 61 access guaranteed. In order to develop their algorithms, competitors also have  
 62 access to 20 known scenarios, 10 without obstacles and 10 with obstacles, all  
 63 different from the ones used during the competition.

64 Based on the best layouts submitted, the competing algorithms are compared  
 65 on each scenario to optimize the cost of energy function. The algorithms are  
 66 ranked on each scenario with a point system provided in Table 1.

Position	1 <sup>st</sup>	2 <sup>nd</sup>	3 <sup>rd</sup>	4 <sup>th</sup>	5 <sup>th</sup>	6 <sup>th</sup>
Points	10	6	4	3	2	1

Table 1: Point system

67 Places below 6<sup>th</sup> receive 0 points. The winner of the competition is the  
 68 competitor that has the highest number of points among the 5 scenarios.

### 69 2.2. Layout evaluation

70 For each layout generated, the goal of the competitors is to minimize the  
 71 cost of energy  $f$  calculated as follows:

$$f = \frac{(c_t n + c_s \lfloor \frac{n}{m} \rfloor) + c_{OM} n}{(1 - (1 - r)^{-y})/r} * \frac{1}{8760P} + \frac{0.1}{n} \quad (1)$$

72 where  $c_t$  is the turbine cost,  $c_s$  is the price of a substation,  $m$  is the number of  
 73 turbines per substation,  $r$  is the interest rate,  $y$  is the farm lifetime in years,  $c_{OM}$   
 74 is the operation and maintenance costs,  $n$  is the number of turbines of the layout,  
 75  $P$  is the layout's energy output. The last term of the fitness function rewards  
 76 layouts with more turbines: without this term, smaller layouts would be more  
 77 optimal, which would be counterproductive with regard to the optimization.

78 This cost function corresponds to the production price of a kilowatt: the  
 79 competitors must produce the layout that minimizes the cost of energy with

80 respect to the scenario provided. Table 2 provides the constant values used in  
 81 the previous equation.

82 Note that a set of constraints must be fulfilled by a wind farm layout to  
 83 be valid. First, all the turbines must be located inside the terrain where the  
 84 wind farm will be deployed, i.e. all turbine positions must be smaller than a  
 85 maximum  $x$  and  $y$  provided in each scenario. Second, the distance between  
 86 turbines must be larger than a given security threshold, which is called  $D_{min}$   
 87 and in our studies was set to 8 times the turbine rotor radius.

Constant	Value
$c_t$	\$750,000
$c_s$	\$8,000,000
$m$	30
$r$	3%
$y$	20 years
$c_{OM}$	\$20,000 per year
$D_{min}$	308m

Table 2: Constant values used in the calculation of the cost of energy.

88 To evaluate the energy output of the wind farm, Kusiak's model has been  
 89 used [1]. It provides the energy output  $P$  of the layout generated by the com-  
 90 petitor optimizers.

### 91 2.3. Inter-turbine interference model

92 The energy capture for a turbine takes into account the following:

- 93 • *Wind Scenario*: Wind speed,  $v$ , represented as a random variable with  
 94 a Weibull distribution that is a summary of wind speed at that location for  
 95 a period of time. This is given by  $p_v(v; c, k|\theta)$ , where  $c$  and  $k$  are  
 96 Weibull shape and scale parameters and  $\theta$  is a wind directional bin. The  
 97 wind speed distribution is different for different directional bins,  $\theta$ . Addi-  
 98 tionally, wind flows from a certain direction with some probability  $p(\theta)$ .  
 99 Together  $p_v(v; c, k|\theta)$  and  $p(\theta)$  are referred to as wind resource/scenario  
 100 in this paper.
- 101 • *Power curve*: A function  $\eta(v)$ , known as a *power curve*, gives the power  
 102 generated by a turbine for the given wind speed  $v$ . The power curve is  
 103 dependent on the turbine make and model.
- 104 • *Wake effects*: In a particular directional bin, for a given turbine  $i$  located  
 105 at  $x_i, y_i$  a number of other turbines affect the wind it experiences. This  
 106 is called wake effect. Given the other turbines' locations  $x_j, y_j$  for all  
 107  $j \in \{1 \dots i - 1, i + 1 \dots n\}$ , the turbines that affect the particular turbine  
 108 are determined using a *wake* model. This is documented in [1]. If a turbine  
 109 located at  $x_i, y_i$  is in the wake of another turbine located at  $x_j, y_j$  in a  
 110 given direction, the wind speed distribution experienced by the turbine

111 is modified by changing the parameter  $c$  resulting in a turbine specific  
 112  $c_i|\theta$ . The value  $c_i < c$  is reduced in proportion to the Euclidean distance  
 113 between  $i$  and  $j$ .

114 To evaluate the energy capture, the objective function needs the *expected*  
 115 value of the energy capture for a given wind resource and turbine positions. For  
 116 a single turbine at position  $(x_i, y_i)$ , it first determines its modified wind resource  
 117 for each directional bin based on other turbine positions and then calculates its  
 118 energy capture using:

$$E = \int_{\theta} p(\theta) \int_v p_v^{\theta}(v; c_i, k_i|\theta) \eta(v). \quad (2)$$

119 Equation 2 evaluates the overall average energy over all wind speeds for a  
 120 given wind direction, and then averages this energy over all wind directions.  
 121 Energy is calculated for every turbine and then summed together to give global  
 122 energy capture.

#### 123 2.4. Framework

124 In order to reduce the competitors' development efforts, we have developed  
 125 an open-source API, called WindFLO, that implements the cost function (and  
 126 the inter-turbine interference model) in multiple languages (C++, Java, Matlab

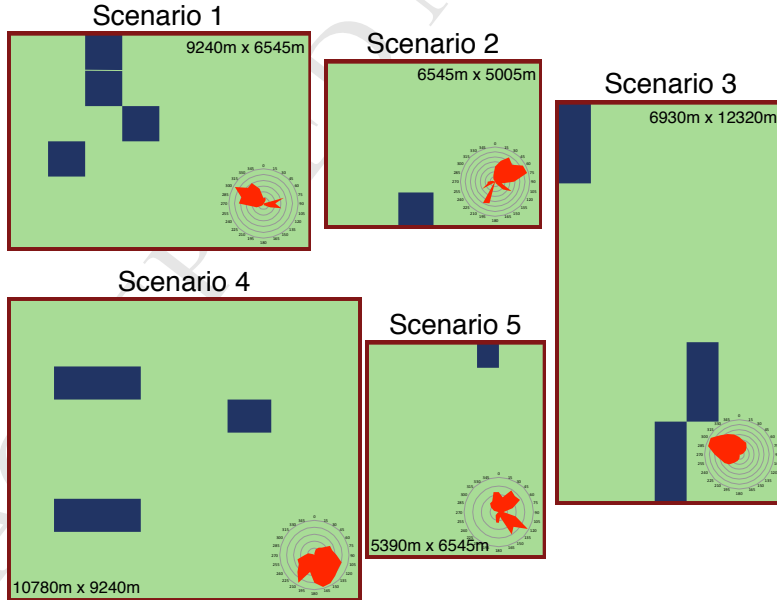


Figure 1: The 5 unknown scenarios used to evaluate the competitors' algorithms. Obstacles are represented with dark blue rectangles.

127 and Python)<sup>1</sup>. The API provides a simple GA as an example of use of the  
128 library.

129 *2.5. Wind scenarios*

130 Figure 1 depicts the scenarios (terrain sizes, obstacles and wind roses) used  
131 to evaluate the competitors' algorithms. Wind roses graphically represent the  
132 wind repartition in force and probability in each direction. These scenarios can  
133 be downloaded from the WindFLO repository.

---

<sup>1</sup>This API is available on github: <https://github.com/d9w/WindFLO>

### 134 3. Competitors' algorithms

135 The second edition of the competition received a total of 8 submissions.  
 136 This section presents the top four approaches. In our opinion, they are the  
 137 most relevant to the wind farm optimization community and provides the best  
 138 results in term of quality of layouts obtained. These four algorithms are available  
 139 in the WindFLO API presented above. These algorithms are the following:

- 140 1. *3s-MDE*: from Carlos Segura, Guillermo López Buenfil, Mario Ocampo  
 141 Pineda, Sergio Ivvan Valdez Peña, Salvador Botello Rionda, and Arturo  
 142 Hernández-Aguirre. The [3-Stages Memetic Differential Evolution \(3s-](#)  
 143 [MDE\)](#) starts by creating a surrogate model which approximates the cost  
 144 function. Then, a memetic differential evolution is used to pre-optimize  
 145 the model based on a geometric distortion of a layout based on rhomboids.  
 146 The pre-optimized layout is then refined by locally modifying the candi-  
 147 date solution. The more accurate model is used only to evaluate solutions  
 148 with a promising behaviour in the surrogate model.
- 149 2. *CMA-ES*: from Ilya Loshchilov and Frank Hutter, this second approach  
 150 uses the Covariance Matrix Adaptation Evolution Strategy (CMA-ES) to  
 151 optimize a layout described by 5 variables: scale (horizontal and vertical),  
 152 shift from the origin, rotation, and shift from a given location.
- 153 3. *SSHH*: from Ahmed Kheiri and Ed Keedwell, [the Sequence-based Selec-](#)  
 154 [tion Hyper-Heuristic \(SSHH\) approach](#) discretized the layout and then  
 155 a solution is represented by three integer variables that corresponds to  
 156 the distance between neighbouring turbines and a shift factor. A hidden  
 157 Markov model produces a sequence of low level heuristics which create the  
 158 final layout.
- 159 4. *GM*: from Brian Goldman, [the Goldman Method \(GM\)](#) presented in this  
 160 paper uses a pair of lattice vectors to calculate turbine locations. It  
 161 also uses the cost of substation, which is larger than the turbine cost  
 162 itself, to leverage the size of the evaluated layouts. A deterministic best-  
 163 improvement local search method is then used to optimize the lattice vec-  
 164 tors.

165 The source codes of these four algorithms are available on the competition  
 166 github: <https://github.com/d9w/WindFLO>. We now discuss these approaches  
 167 in turn.

#### 168 3.1. Memetic Differential Evolution with Surrogate Model and Ad-hoc Improve- 169 ments (3s-MDE)

170 In this section we present a three-stage optimizer — see Algorithm 1 — that  
 171 combines a memetic differential evolution (MDE) with a novel representation of  
 172 candidate solutions, a surrogate model and ad-hoc improvements. This method  
 173 is referred to as 3S-MDE in the rest of the paper. A detailed flowchart of the  
 174 scheme describing the three stages is given in Fig. 2. In this flowchart, the boxes  
 175 that perform evaluations in the real simulator — in contrast to those that use  
 176 the surrogate model — are shown in gray. The following sections describe each  
 177 stage of this optimizer.



**Algorithm 1** Memetic DE with Surrogate Model and Ad-hoc Improvements

- 1: **Stage 1:** Create a Surrogate Model  $SM$ .
- 2: **Stage 2:** Apply a memetic DE/rand/1/bin using  $SM$  with a representation based on rhomboids.
- 3: **Stage 3:** Apply ad-hoc improvements to the best solution obtained in Stage 2.

178 *3.1.1. First Stage: Construction of a Surrogate Model*

179 One of the main difficulties when dealing with complex engineering problems  
 180 is that evaluating a solution is usually quite an expensive process. Surrogate  
 181 models can be used to alleviate this difficulty [17]. Different ways of build-  
 182 ing surrogate models have been proposed. Problem-dependent models rely on  
 183 ad-hoc knowledge of the problem, whereas with problem-independent models,  
 184 machine learning methods are usually employed [18].

185 For this optimizer, a problem-dependent surrogate model is built to approx-  
 186 imate the energy generated by a given set of turbines. In order to construct  
 187 the surrogate model, a set of simple candidate solutions where only two tur-  
 188 bines are placed in the wind farm are evaluated using the original evaluator.  
 189 **Additionally, one evaluation with a single turbine is carried out to estimate the**  
 190 **maximum energy that it can generate.** For each evaluation with two turbines,  
 191 the penalty on the energy produced in both turbines with respect to the case  
 192 where only one turbine is placed in the wind farm is calculated. Specifically, the  
 193 following set of distances are checked:  $D_{min}$ ,  $1.5D_{min}$ ,  $2D_{min}$ ,  $2.5D_{min}$ ,  $3D_{min}$   
 194 and  $3.5D_{min}$ , where  $D_{min}$  represents the minimum admissible distance between  
 195 turbines. For the case in which the distance between turbines is set to  $D_{min}$ ,  
 196 720 equidistributed different angles are checked, whereas in the remaining cases,  
 197 360 different angles are used.

198 The surrogate model uses the saved data to approximate the energy gener-  
 199 ated by layouts that use any number of turbines. The model assumes that  
 200 the energy generated by one turbine is not influenced by any other turbines  
 201 placed further away than  $3.5D_{min}$ . Thus, for each turbine, the set of conflicting  
 202 turbines — those at a distance not greater than  $3.5D_{min}$  — is detected and  
 203 the negative influence is estimated based on the saved data. Specifically, if for  
 204 a given turbine there exists another turbine at a distance  $D$  and angle  $\gamma$ , then  
 205 the four surrounding cases — combining the nearest distances and angles — are  
 206 identified and linear interpolations are used to estimate the negative influence.  
 207 Note that the computational complexity of identifying the surrounding cases  
 208 with values higher and lower than  $D$  and  $\gamma$  is constant, so this process is quite  
 209 fast. The total energy generated by a given turbine is the estimate of the maxi-  
 210 mum attainable energy minus the sum of the estimated negative influences. The  
 211 total energy estimated for a given layout is the sum of the energies estimated  
 212 for each turbine.

213 *3.1.2. Second Stage: Memetic Differential Evolution*

214 In the second stage, one of the most well-known variants of DE is applied.  
 215 Specifically, the DE/rand/1/bin is used [19]. This variant has the property of

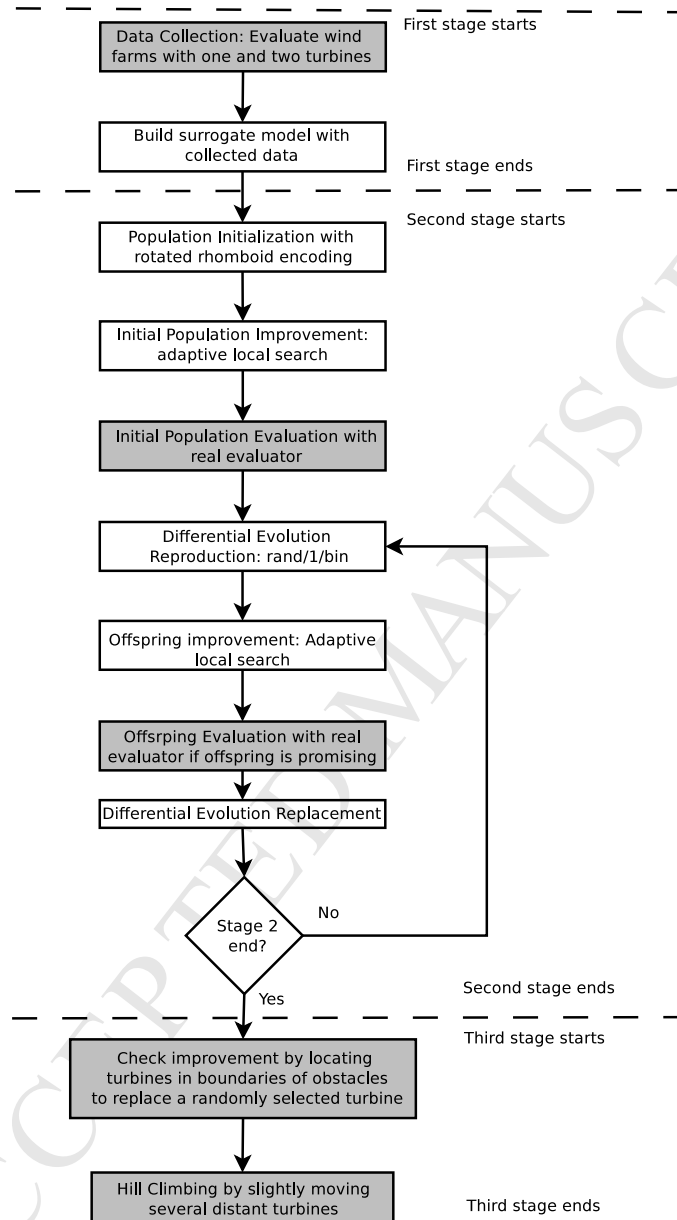


Figure 2: 3s-MDE Flowchart

216 being more explorative than schemes that apply the “best” strategy. This fea-  
 217 ture was vitally important due to the small population size ( $N$ ) used in the  
 218 runs. In the current MDE implementation, a special initialization of the popu-  
 219 lation is used. First, 200 individuals are created; then, the best  $N$  individuals

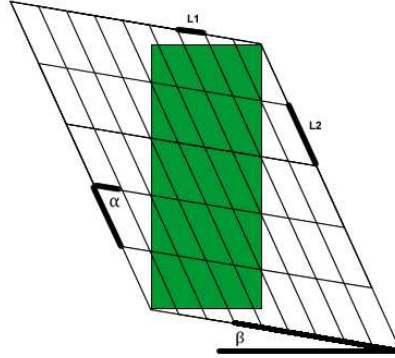


Figure 3: Encoding of Individuals in MDE

220 are selected to form the initial population.

221 One of the keys to designing proper Evolutionary Algorithms (EAs) is the  
 222 selection of a suitable encoding of the individuals [20]. Directly encoding the  
 223 coordinates of the turbines yields too large a search space, thus an alternative  
 224 encoding was adopted. Specifically, a solution is encoded with four real-valued  
 225 parameters, which establish the geometry of a possibly rotated rhomboid (see  
 226 Figure 3):  $L1$  and  $L2$  are the lengths of the sides of the rhomboid;  $\alpha$  is the  
 227 angle formed between two sides of the rhomboid; finally,  $\beta$  rotates the whole  
 228 rhomboid. This rhomboid is used to establish the positions where the turbines  
 229 are deployed, which is illustrated in Figure 3. Specifically, the given scenario —  
 230 green zone — is covered with a set of rhomboids with the specified geometry  
 231 and the turbines are positioned at the vertexes of these rhomboids. One of the  
 232 vertexes of the rhomboids is placed in the bottom-left corner of the wind farm.  
 233 Since some turbines might be too close to one another, a repairing method is  
 234 used to remove conflicting turbines. First, the turbines are randomly shuffled.  
 235 Then, each turbine is sequentially examined and is accepted only if it does not  
 236 conflict with any previously accepted turbine, i.e. it is accepted if the distance  
 237 to any already selected turbine is not smaller than  $D_{min}$ . Additionally, when a  
 238 vertex is inside an obstacle, no turbine is located in such a vertex.

239 In order to improve upon the intensification capabilities, DE was integrated  
 240 with an adaptive local search, which is applied both in the creation of the initial  
 241 population and after the creation of the offspring. The number of evaluations  
 242 used in each application of the local search is set with the local search budget  
 243 ( $LSB$ ) parameter. The adaptive search starts with a given step size ( $SS$ ) for  
 244 each parameter which is progressively decreased linearly with the aim of in-  
 245 creasing the intensification capabilities. The reduction is calculated in such a  
 246 way that by the end of the local search the resulting value is 0. When each  
 247 neighbor is created, any of the four parameters is changed with a probability  
 248 equal to 0.25. Specifically, they are modified by summing or subtracting the  
 249 step size corresponding to the iteration. Note that applying the real evaluator

250 in the local search would be very expensive. As a result, the adaptive local  
 251 search uses the surrogate model and only the best solution obtained after the  
 252 application of each local search might be evaluated with the original evaluator.  
 253 Specifically, the obtained solution is evaluated with the original evaluator only  
 254 if it is not worse than 1.20 multiplied by the best so far obtained fitness. Thus,  
 255 the surrogate model is also used to filter out poor solutions, which is a typical  
 256 use of surrogates.

### 257 3.1.3. Third Stage: Ad-hoc Improvement

258 The last stage starts from the best solution identified by the memetic DE  
 259 and applies two methods to further improve it. Note that in this last phase,  
 260 the surrogate model is not used because some minor modifications are made  
 261 to the candidate solutions, thus making it impossible to properly measure the  
 262 promising behavior of these changes with the surrogate model.

263 The first method is applied only in the scenarios where obstacles are in-  
 264 cluded. First, given a budget  $B$  for evaluations,  $\frac{B}{2}$  potential locations are  
 265 identified. Specifically, at each edge of the obstacles,  $\frac{B}{N_{OBS} * 4 * 2}$  locations are  
 266 equidistributed, where  $N_{OBS}$  is the number of obstacles. Then, for each se-  
 267 lected location, a new solution is evaluated that considers the establishment of  
 268 a turbine in that position and the removal of a randomly selected turbine. The  
 269 modification is maintained only if the fitness is improved.

270 Finally, the remaining evaluations are used to apply a local search. In the  
 271 initial version of the local search, neighbors were generated by slightly moving a  
 272 single turbine. Specifically, a maximum step ( $MS$ ) was established — here set to  
 273 6.25 units — and in order to generate a neighbor, a turbine was moved  $S$  units,  
 274 where  $S$  was a randomly generated number between 0 and  $MS$ . The direction of  
 275 movement was also randomly generated. Given that the number of evaluations  
 276 is very restricted, instead of moving a single turbine, the local search moves  
 277 several turbines simultaneously, following the same method explained above.  
 278 Distant turbines are selected using the process below. First, a safety distance  
 279 ( $SD$ ) is established to  $6 \times D_{min}$ . Then, a turbine present in the current solution  
 280 is randomly selected and a grid of square cells with a side length equal to  $SD$   
 281 is set up in the wind farm in such a way that the center of a cell is in the  
 282 position of the selected turbine. Then, for each cell, the turbine that is closest  
 283 to the center is selected. In this way, a set of distant turbines is generated. The  
 284 new candidate solution is created by moving each selected turbine. Then, the  
 285 energy generated in each cell is calculated and the cells where the amount of  
 286 energy generated is increased are considered to be promising moves. Finally,  
 287 the movements involving unsuccessful cells are undone and the new candidate  
 288 solution is reevaluated. If the fitness of the new solution improves the original  
 289 solution, it is accepted. This process is repeated until the budget for the number  
 290 of evaluations is exhausted.

### 291 3.1.4. Parameterization

292 3S-MDE needs a set of parameters, which were tuned with the set of instances  
 293 given in the first part of the contest. Table 3 provides the parameters used in

294 this competition.

Parameter name	Notation	value
Population size	$N$	10
Crossover rate	$CR$	0.9
Mutation scale factor	$F$	Gaussian dist. $\mathcal{N}(0.5, 0.3)$
L1 Step size	$L1\text{-SS}$	125
L2 Step size	$L2\text{-SS}$	125
$\alpha$ Step Size	$\alpha\text{-SS}$	22.5 degrees
$\beta$ Step Size	$\beta\text{-SS}$	22.5 degrees
Local search budget (Initialization)	I-LSB	15000
Local Search budget (Offspring)	O-LSB	5000
Criterion to pass to third stage	N/A	90% of Evaluations

Table 3: Parameters of the 3s-mde method.

### 295 3.2. CMA-ES for layout optimization (CMA-ES)

296 The Covariance Matrix Adaptation Evolution Strategy (CMA-ES) [21] is  
 297 the method of choice when dealing with hard black-box optimization problems  
 298 which are nonlinear, multimodal and/or noisy. The algorithm is invariant to  
 299 rank-preserving transformations of the objective function and affine transforma-  
 300 tions of the search space which makes it parameter-less in practice. CMA-ES  
 301 has repeatedly demonstrated good performance at various platforms for compar-  
 302 ing continuous optimizers such as the Black-Box Optimization Benchmarking  
 303 (BBOB) workshop [22, 23, 24] and the Special Session at Congress on Evo-  
 304 lutionary Computation [25, 26]. Thus, CMA-ES seems naturally suitable for  
 305 the wind farm layout optimization problem especially when a low-dimensional  
 306 parameterization of the design problem is considered.

307 In this section, we discuss the application of CMA-ES to the wind farm  
 308 layout optimization problem. In a nutshell, CMA-ES works as follows. In its  
 309 iteration  $t$ , a mean  $m^t$  of the mutation distribution (which can be interpreted  
 310 as an estimation of the optimum) is used to generate  $\lambda$  candidate solutions  
 311  $x_k \in \mathbb{R}^n$  by adding a random Gaussian mutation defined by a (positive definite)  
 312 covariance matrix  $C^t \in \mathbb{R}^{n \times n}$ . The  $k$ -th sampled candidate solution  $x_k^t$  is then  
 313 defined as:

$$x_k^t \sim \mathcal{N}(m^t, \sigma^{t^2} C^t) = m^t + \sigma^t \mathcal{N}(0, C^t), \quad (3)$$

314 where  $\sigma^t$  is a mutation step-size. These  $\lambda$  solutions then should be evaluated  
 315 on an objective function  $f$ . The old mean of the mutation distribution is stored  
 316 in  $m^t$  and a new mean  $m^{t+1}$  is computed as a weighted sum of the best  $\mu$  parent  
 317 individuals selected among the  $\lambda$  generated offspring individuals. The algorithm  
 318 adapts  $m^t$  and  $C^t$  in order to increase the likelihood of the successful sampling  
 319 steps to appear again and to proceed towards the optimum.

320 Since we optimize both the number of turbines and their positions, the di-  
 321 rect representation of turbine positions as variables would lead to a large-scale

Parameter	Notation	Optimized
Layout height	$H$	No (input)
Layout width	$W$	No (input)
Turbine radius	$R$	No (input)
Layout scale factor	$h_1$	No, fixed to 4
Interturbine scale on x-axis	$h_2$	No, fixed to 4
Interturbine scale on y-axis	$h_3$	No, fixed to 4
Interturbine distance on x-axis	$x_1$	Yes
Interturbine distance on y-axis	$x_2$	Yes
Rotation angle	$x_3$	Yes
Shift on x-axis	$x_4$	Yes
Shift on y-axis	$x_5$	Yes

Table 4: Parameters optimized with CMA-ES and constants used in this approach.

322 optimization problem which is often intractable [13]. Similarly to other algo-  
323 rithms presented in this paper, we therefore parameterize the search space of  
324 wind-farm layouts with only a few variables. We use 5 continuous variables to i)  
325 fill a rectangular grid of turbines, ii) shift it to the origin, iii) rotate it, and then  
326 iv) shift it to some location. Finally, all turbines which violate the constraints  
327 (e.g., obstacles, target size of the layout) are removed from the grid.

328 We parameterize the original optimization problem as follows:

329 **STEP 1** The initial rectangular grid is selected to be  $h_1 = 4$  times larger than the  
330 maximum size ( $W; H$ ) of the target layout to take into account its rotation  
331 in STEP 2. The minimum distance between turbines on the x-axis is set  
332 by  $D_x = D_{min} + (0.2x_1)^{h_2} \times (W - D_{min})$ , where  $D_{min} = 8R$  and  $h_2$   
333 is a hyperparameter set to 4. Similarly, the distance on y-axis is set by  
334  $D_y = D_{min} + (0.2x_2)^{h_3} \times (H - D_{min})$ . Thus, the total number of turbines  
335 is  $(\lfloor h_1 \times W/D_x \rfloor + 1)(\lfloor h_1 \times H/D_y \rfloor + 1)$ .

336 **STEP 2** Shift the grid to the origin by subtracting  $(h_1 \times W/2; h_1 \times H/2)$  and  
337 rotate turbine coordinates by an angle  $\theta = -\pi + 2\pi x_3$ .

338 **STEP 3** Shift the rotated grid by  $((0.5 + 0.2x_4) \times W; (0.5 + 0.2x_5) \times H)$ .

339 **STEP 4** Remove all infeasible turbines.

340 Table 4 summarizes the various constants used as well as the five variables  
341  $x_1$  to  $x_5$  optimized by CMA-ES. All these 5 variables are constrained to be in  
342  $[0, 1]$  and are optimized with the active CMA-ES [27, 28] in its default settings  
343 and with  $m^0 = [0.5]^5$  and  $\sigma^0 = 0.3$ .

### 344 3.3. A Sequence-based Selection Hyper-heuristic (SSHH)

345 In contrast to the other techniques, hyper-heuristics operate at the level  
346 above (meta-)heuristics such as EAs. Selection hyper-heuristics are high level  
347 control methods that mix and manage a predefined set of low level heuristics  
348 for solving hard computational problems. Hence, online learning is a crucial  
349 component of such methods which are capable of discovering the appropriate

350 combinations of low level heuristics yielding an improved overall performance.  
 351 More on different types of hyper-heuristics, including an overview of different  
 352 algorithmic components and designs, and their applications can be found in [29].

353 Traditionally, a selection hyper-heuristic employs two methods, consecu-  
 354 tively: a *heuristic selection* method to choose a suitable low level heuristic (move  
 355 operator) which is applied to a candidate solution, and then a *move acceptance*  
 356 method to decide whether to accept or reject the newly generated solution. This  
 357 study presents a sequence-based selection hyper-heuristic (SSHH) consisting of  
 358 a learning sequence of heuristics selection method and an adaptive threshold  
 359 move acceptance method to solve the wind farm layout optimization problem.

### 360 3.3.1. Representation and overall search

361 In order to pick the best locations for a set of turbines, a given region is split  
 362 into a grid consisting of a certain number of rows and columns with neighbour-  
 363 ing cells having an interval of size  $(0.1 \times \text{TurbineRadius})$  in between them. A  
 364 given solution is represented using three integer variables,  $X$ ,  $Y$  and  $S$ , where  
 365  $M \leq X < \text{maxCols}$ ,  $M \leq Y < \text{maxRows}$ , and  $0 \leq S$ ;  $M$  is the minimum al-  
 366 lowed distance between neighbouring turbines,  $\text{maxRows}$  and  $\text{maxCols}$  are the  
 367 maximum number of rows and columns, respectively (see Figure 4). Based on  
 368 the values of those variables, a binary matrix is formed by spreading neighbour-  
 369 ing turbines with a separating distance of  $X$  cells at each row and a separating  
 370 distance of  $Y$  cells at each column. A cyclic shift is performed at each row start-  
 371 ing from the second row. The  $S$  parameter is used to reduce the wake effect  
 372 from a neighbouring turbine and deals with differing wind directions by shift-  
 373 ing wind turbines. Algorithm 1 provides the pseudocode of how the solution is  
 374 constructed.

---

**Algorithm 1:** The pseudocode of how a solution is constructed

---

```

input : scenario,  $X$ ,  $Y$  and  $S$ 
output: grid
1 for  $i \leftarrow 0; i < \text{maxCols}; i += X$  do
2   for  $j \leftarrow 0; j < \text{maxRows}; j += Y$  do
3      $l = (i + (j/Y) * S) \% \text{maxCols};$ 
4     if scenario.isValidLocation(l, j) then
5       grid.insertTurbineAtLocation(l, j);
6     end
7   end
8 end

```

---

375 SSHH performs the search under an iterative framework maintaining the  
 376 best solution detected so far. Solutions are always made feasible by removing  
 377 the invalid turbines which are placed on obstacles, before evaluation.

### 378 3.3.2. Low level heuristics

379 The low level heuristics (LLHs) used in this work are parameterized low  
 380 level heuristics. Assume that  $H(V_1, p, V_2)$  is a heuristic, where  $p$  has one of

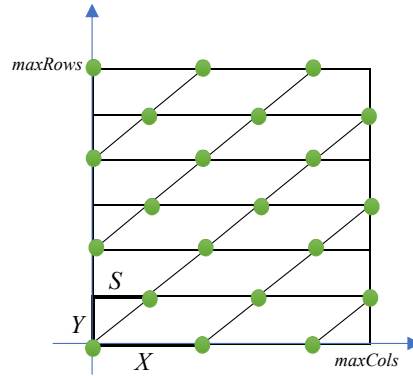


Figure 4: Encoding of Individuals in SSHH

381 three values: 1,  $\text{rand}[1,10]$  or  $\text{rand}[10,79]$ ; and  $\text{rand}[L, U]$  is a random integer  
 382 in  $[L, U]$  and this low level heuristic modifies (increases or decreases) the value  
 383 of the variable  $V_1$  by  $p$ , and then with a probability of 0.30 resets the value  $V_2$ .  
 384 SSHH controls the following low level heuristics during the search process:

- 385 • **LLH0:** Apply  $H(X, p, S)$
- 386 • **LLH1:** Apply  $H(Y, p, S)$
- 387 • **LLH2:** Apply  $H(S, p, X)$ , then with a probability of 0.30 reset the value  
 388 of  $Y$ .
- 389 • **LLH3:** increase or decrease the value of  $X$  by  $p$ ; then update  $p$  and apply  
 390  $H(Y, p, S)$ .
- 391 • **LLH4:** increase or decrease the value of  $X$  by  $p$ ; then update  $p$  and  
 392 increase or decrease the value of  $Y$  by  $p$ ; and finally update  $p$  and increase  
 393 or decrease the value of  $S$  by  $p$ .

### 394 3.3.3. Heuristic sequence selection and move acceptance

395 The selection component forms and applies a sequence of low level heuristics  
 396 to a candidate solution as a single operation, thereby generating super-  
 397 heuristics through the combination of more than one low level heuristic. This  
 398 online learning method analyses and produces sequences of heuristics during  
 399 the search process using a hidden Markov model, in which the hidden states  
 400 are low level heuristics (LLHs) and observations are sequence-based acceptance  
 401 strategies (AS). We make use of two matrices: a transition probability matrix to  
 402 determine the movement between states and an emission probability matrix to  
 403 determine whether the sequence of heuristics that has been constructed will be  
 404 applied to a candidate solution or that sequence will be extended by including  
 405 another LLH. As explained earlier, each heuristic is associated with a parame-  
 406 ter,  $p$  influencing its behaviour. Therefore, an additional emission probability



407 matrix is implemented to set the value of  $p$ . A detailed description of this al-  
 408 gorithm can be found in [30, 31, 32]. The threshold move acceptance method  
 409 accepts all improving moves by default. However, the non-improving moves are  
 410 accepted only if the cost of the new solution is less than or equal to a threshold  
 411 which changes with respect to the best solution during the search process. The  
 412 threshold is always set to the (1.01) of the cost of the best solution found so far,  
 413 whenever a non-improving move occurs.

#### 414 3.4. The Goldman Method (GM)

##### 415 3.4.1. Representation

416 There are two straightforward approaches to representing turbine locations  
 417 in the field, both of which have significant limitations.

418 The first method would be to enforce a maximally compact two-dimensional  
 419 mesh, with each mesh point representing a possible turbine. This method han-  
 420 dles obstacles gracefully as invalid mesh points can be removed before beginning  
 421 search. As search focuses on which mesh points to include as turbines, the total  
 422 number of turbines in the field is easy to manipulate. However, the mesh struc-  
 423 ture does not allow turbines to orient themselves with the wind. For example,  
 424 it is possible that the wind is blowing parallel to one of mesh axes, resulting in  
 425 all turbines in a row (or column) interfering with each other.

426 The second method would be to specify some number of turbines and then  
 427 search their possible locations in the field. While this can overcome the problem  
 428 of interference, it massively increases the search space. Furthermore, it now  
 429 becomes challenging to determine the correct number of turbines to use and to  
 430 avoid obstacles.

431 In an attempt to gain the best of both techniques, while simultaneously re-  
 432 ducing the search space size, the Goldman method represents a layout as two  
 433 vector lattice. In this form, search is performed over the space of a pair of  
 434 two-dimensional vectors. These vectors are converted to a layout by placing a  
 435 turbine at all integer linear combinations of the two lattice vectors. As with  
 436 the mesh representation any invalid turbine is removed, resulting in simple ob-  
 437 stacle handling. Yet unlike that method turbines can orient at any angle to  
 438 each other, with a flexible amount of space between each, to avoid interference.  
 439 To aid search, the Goldman method encodes the two lattice vectors as (angle,  
 440 magnitude) pairs.

##### 441 3.4.2. Number of Turbines

442 A significant cost of any layout is how many substations must be purchased.  
 443 The cost of energy function includes the term  $c_s * \lfloor \frac{N}{M} \rfloor$ . The cost of a substation,  
 444  $c_s$ , is an order of magnitude larger than the cost of a turbine. As a result the  
 445 cost of energy is often minimized when  $N \bmod M = M - 1$  as this uses the  
 446 maximum number of turbines before a new substation must be purchased.

447 The Goldman method leveraged this knowledge when evaluating layouts.  
 448 Along with calculating the global cost of energy, each evaluation provides the  
 449 user with information about the “fitness” of individual turbines in the layout.

450 The Goldman method used this information to reduce each tested layout to  
 451 the nearest complete substation by naïvely removing the least fit turbines. The  
 452 reduced layout is then evaluated, meaning that every lattice requires at most  
 453 two evaluations.<sup>2</sup> The lattice’s cost of energy is then considered to be whichever  
 454 version was cheaper.

### 455 3.4.3. Search Method

456 Given the limited evaluation budget, the Goldman method utilizes a deter-  
 457 ministic best-improvement local search method to explore the space of lattice  
 458 vectors. To simplify this process and further reduce the search space, the four  
 459 variables (two angles and two magnitudes) which encode the lattice were dis-  
 460 cretized. Angles were restricted to 36 intervals spaced  $\pi/18$  apart. Magnitudes  
 461 ranged from the minimum allowable interval between turbines up to 5 times  
 462 that size in 64 evenly spaced steps.

463 To perform local search, the algorithm began from a lattice with the vectors  
 464 perpendicular to each other, one using the minimum magnitude and the other  
 465 using the middle of the magnitude range. All alternatives to each variable were  
 466 then tested sequentially, such that only the best changing improvement to a  
 467 variable is made before continuing to the next variable. This process continues  
 468 until no single variable can be changed to make the lattice better. To improve  
 469 rotational symmetry, this process is run starting with the long vector parallel  
 470 to the x-axis, and then again parallel to the y-axis. Duplicate work is prevented  
 471 by caching the quality of each discrete lattice.

---

<sup>2</sup>Some lattices create layouts where  $N \bmod M = M - 1$

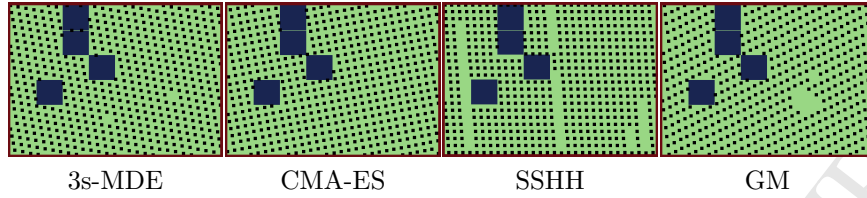


Figure 5: Best layouts obtained by the 4 competitors on scenario 1.

#### 472 4. Competition results

##### 473 4.1. Competition results

474 The algorithms presented in the previous section, in addition to four others  
 475 not described in this paper, were run on the 5 scenarios presented in the competi-  
 476 tion rules section. As mentioned above, the competitors were given a budget  
 477 of 10,000 evaluations to split between the 5 scenarios for computational cost  
 478 reasons. Table 5 provides the costs of energy fitness of each algorithms. As a  
 479 basis of comparison, we have compared the results to a genetic algorithm. GAs  
 480 have been used many times in this domain and offer a familiar and standard  
 481 benchmark against other algorithms from the field of evolutionary computation.  
 482 For this problem, a GA optimizes a binary genome that decides whether or not  
 483 a turbine is located in each grid of a discretized layout. The fitness function  
 484 used to evaluate each layout is the one presented in equation 1. The GA is set  
 485 up with a population size of 20 individuals, a 4-player tournament selection with  
 486 elitism, 5% mutation and 40% crossover. Mutating a layout consists in switch  
 487 a Boolean of the grid and crossing is a standard one-point crossover. The GA  
 488 is run for 50 generations, which represents 2000 evaluation per scenario.

489 Table 7 provides both the number of turbines and of substations of the best  
 490 layouts obtained by the different competitors on the different scenarios. It is  
 491 worth noting that obtained layouts are of comparable size in terms of number  
 492 of turbines for each scenario. Also, the algorithms, either naturally or due to  
 493 specific strategies, limit the number of turbines to a value very close to the con-  
 494 straints of the substations. When evaluating the cost of energy function, the  
 495 cost of building a substation is subsequently greater than the total price of the  
 496 turbines. Therefore, the number of substations, even though not directly high-  
 497 lighted in the problem description, is of primary importance. Figure 5 depicts

Scenario	3s-MDE	CMA-ES	SSHH	GM	GA
1	<b>1.16</b> <sub>4422</sub> $E^{-3}$	1.17 <sub>2731</sub> $E^{-3}$	1.18 <sub>1129</sub> $E^{-3}$	1.18 <sub>5466</sub> $E^{-3}$	1.26 <sub>9266</sub> $E^{-3}$
2	<b>1.00</b> <sub>929</sub> $E^{-3}$	1.02 <sub>9998</sub> $E^{-3}$	1.03 <sub>9825</sub> $E^{-3}$	1.04 <sub>4906</sub> $E^{-3}$	1.15 <sub>8464</sub> $E^{-3}$
3	<b>6.26</b> <sub>867</sub> $E^{-4}$	6.30 <sub>916</sub> $E^{-4}$	6.40 <sub>241</sub> $E^{-4}$	6.49 <sub>096</sub> $E^{-4}$	6.91 <sub>265</sub> $E^{-4}$
4	6.53 <sub>861</sub> $E^{-4}$	<b>6.53</b> <sub>56</sub> $E^{-4}$	6.66 <sub>205</sub> $E^{-4}$	6.64 <sub>341</sub> $E^{-4}$	7.18 <sub>626</sub> $E^{-4}$
5	<b>1.14</b> <sub>2309</sub> $E^{-3}$	1.15 <sub>2661</sub> $E^{-3}$	1.16 <sub>7168</sub> $E^{-3}$	1.16 <sub>033</sub> $E^{-3}$	1.26 <sub>9238</sub> $E^{-3}$

Table 5: Cost of energy, compared to the state-of-the-art layout optimization (binary GA).

Scenario	3s-MDE	CMA-ES	SSHH	GM	GA
1	10	6	4	3	-
2	10	6	4	3	-
3	10	6	4	3	-
4	6	10	3	4	-
5	10	6	3	4	-
Total	46	34	18	17	-
Rank	1 <sup>st</sup>	2 <sup>nd</sup>	3 <sup>rd</sup>	4 <sup>th</sup>	-

Table 6: Competition results in points and ranking. Note that GA was not part of the competition and is therefore not ranked. The results of other competitors are not presented in this table.

Scenario	#Turbines				#Substations			
	3s-MDE	CMA-ES	SSHH	GM	3s-MDE	CMA-ES	SSHH	GM
1	539	539	561	479	18 <sup>(0)</sup>	18 <sup>(0)</sup>	19 <sup>(-8)</sup>	16 <sup>(0)</sup>
2	388	239	329	324	13 <sup>(-1)</sup>	8 <sup>(0)</sup>	11 <sup>(0)</sup>	11 <sup>(-5)</sup>
3	899	804	809	680	30 <sup>(0)</sup>	27 <sup>(-5)</sup>	27 <sup>(0)</sup>	23 <sup>(-9)</sup>
4	929	929	958	898	31 <sup>(0)</sup>	31 <sup>(0)</sup>	32 <sup>(-1)</sup>	30 <sup>(-1)</sup>
5	359	358	348	356	12 <sup>(0)</sup>	12 <sup>(-1)</sup>	12 <sup>(-1)</sup>	12 <sup>(-3)</sup>

Table 7: Number of turbines and of substations of the best layouts obtained by the competitors on each scenarios. In the substation part of the table, the value parenthesis represents the number of missing turbines in order to have all substations fully used (30 turbines per substation).

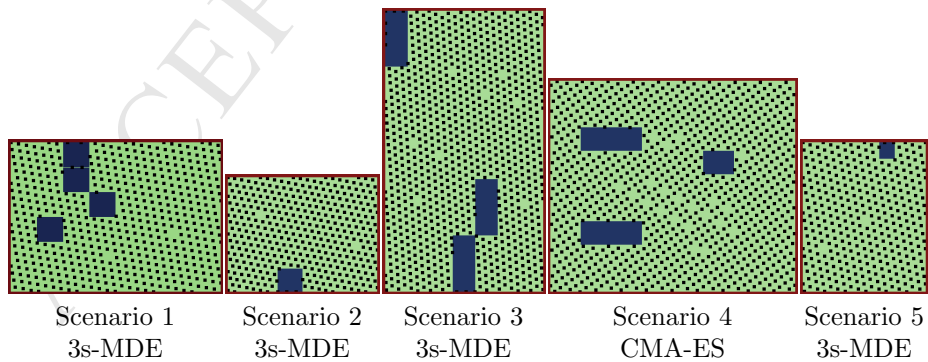


Figure 6: Best layouts obtained on the 5 scenarios.

498 the four layouts obtained by the four competitors for scenario 1. We can note  
499 similarities of the geometric arrangement strategies used by the competitors,  
500 albeit with different approaches, to compress the number of variables induced  
501 by the problem to a lower amount. They mostly operate on a transformation  
502 (shift, scale and rotation) of a grid layout prior to a removal of turbines that  
503 violate constraints (obstacles) and local deletion for layout refinement. Figure  
504 6 presents the best layouts across all competitors obtained for each scenario.  
505 Once again this geometric arrangement strategy appears on the obtained layout  
506 with various rotations and shifts depending on the terrain characteristics.

#### 507 4.2. Convergence comparison

508 Figure 7 shows the convergence curves of the different algorithms. They  
509 represent the competitor algorithms' best evaluations. Each algorithm curve  
510 stops at the final evaluation. As an example, the GA is always used with a fixed  
511 2000 evaluation steps for each scenario.

512 First, the 3s-MDE optimization strategy is noticeable on the plots: whereas  
513 good fitness values appear as soon as the first evaluation in other approaches,  
514 3s-MDE only has competitive fitness values after 1260 evaluations. This corre-  
515 sponds to the duration needed by the algorithm to build the surrogate model.  
516 During this initial phase, the algorithm evaluates layouts with only two turbines,  
517 which generate very poor layouts (not represented in the plot for visualization  
518 purposes).

519 Secondly, it can be noticed that all other algorithms converge in few itera-  
520 tions (approximately 300 evaluations) to a very good solutions before starting  
521 local optimization. Even though 3s-MDE needs more evaluation steps to pro-  
522 duce a good layout, the initial 1260 evaluations are only made with 2 turbines  
523 which is costless in comparison to layouts with hundreds to thousands of tur-  
524 bines. Therefore, we can argue that the layouts can be presented to the farm  
525 designer very early in the optimization loop across all presented methods.

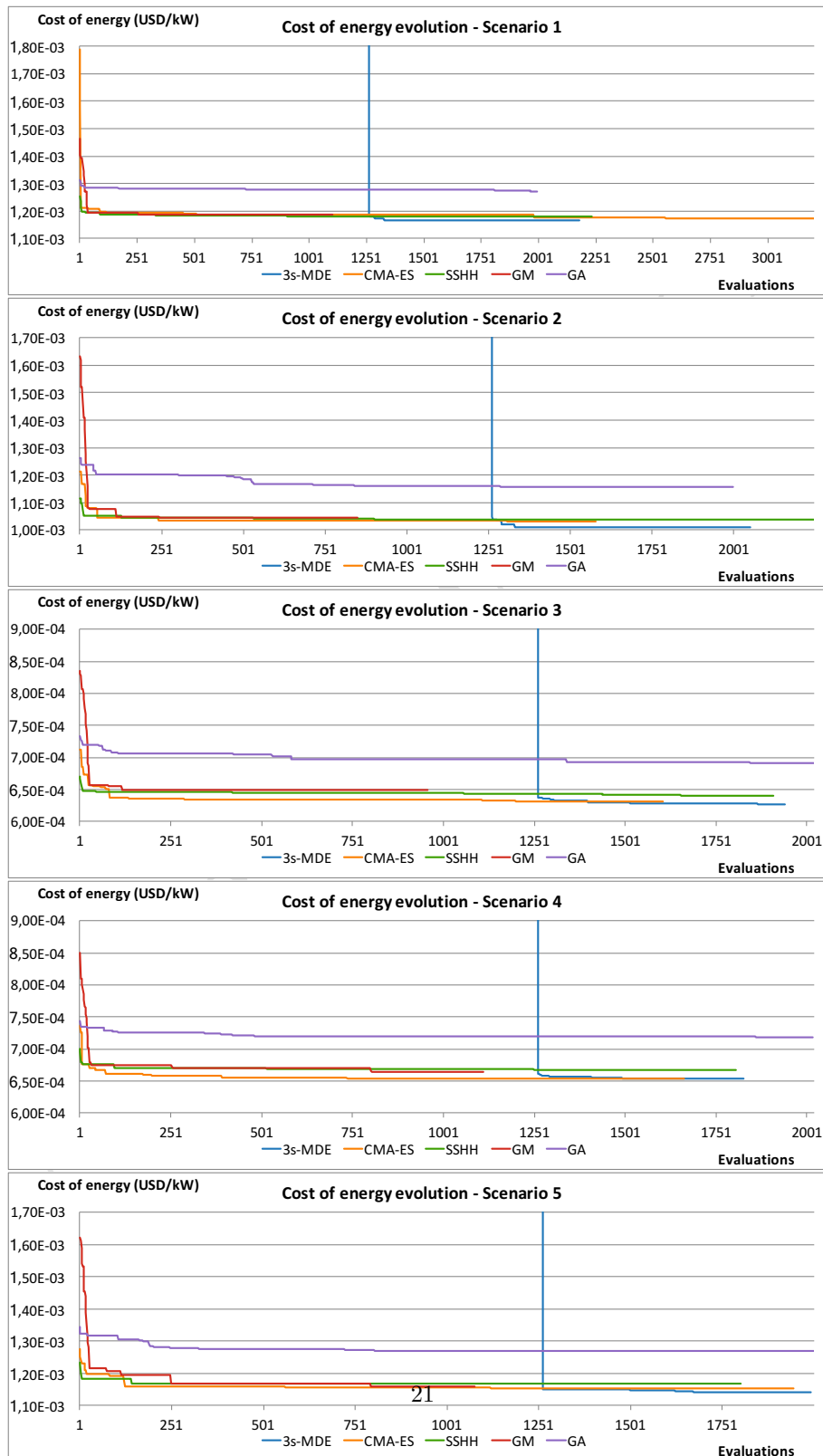


Figure 7: Comparison of the convergence profile of the different algorithms on the 5 scenarios.

## 526 5. Conclusion

527 This paper presented the results of the 2015 competition on wind farm layout  
528 optimization. With this event, we were able to propose innovative algorithms to  
529 optimize large wind farms with a strong computational constraint. Thanks to  
530 this competition, we were also able to compare these approaches with state-of-  
531 the-art algorithms and observe the potential improvement of the optimization  
532 algorithms used to generate the wind farm layouts.

533 This competition also provides a framework to compare future algorithms  
534 with existing ones on a comparative basis. The competition framework is freely  
535 available in multiple programming languages (C++, Java, Matlab and Python)  
536 with a set of randomly generated wind scenarios.

537 Because solutions were obtained with acceptable computational costs in this  
538 competition, we can now imagine targeting new optimization objectives. The  
539 3D structure of the terrain, and/or heterogeneous wind distribution within the  
540 terrain, heterogeneous wind turbines with different height, width and power  
541 curves could be considered. In this competition, cable and road networks were  
542 not taken into account, but these are of great importance for the initial invest-  
543 ment to build the wind farm. They could be added to the framework and the  
544 cost of energy function in order to be addressed by the optimization algorithms.

545 One of the main points we learned from this competition is that the algo-  
546 rithms proposed by the competitors mainly work on optimizing very few pa-  
547 rameters in comparison to state-of-the-art algorithms; instead of optimizing the  
548 Cartesian coordinates of individual turbines, it seems preferable to optimize ge-  
549 ometric parameters. By doing so, the complexity of the search space is drastically  
550 reduced, leading to very acceptable optimization time, even for very large wind  
551 farms. These geometric parameters allow for continuous turbine placement over  
552 the entire grid, which is clearly advantageous over the discrete grid used by the  
553 GA and previously in the literature [15]. Furthermore, these parameters could  
554 be exposed to human wind farm designers to allow them to understand the  
555 optimal placement of turbines based on the wind scenario and the constraints  
556 given to the optimization. Understanding optimized grids such as Figures 3  
557 and 4 would allow human wind farm designers the flexibility of choosing tur-  
558 bine placement while still benefiting from an optimized energy cost.

559 Beyond demonstrating the utility of reducing this problem to an optimiza-  
560 tion of geometric parameters, the successful use of a surrogate model in this  
561 problem is novel and significant. As a surrogate could be built using gathered  
562 wind data a single time before layout design starts, the computational load of  
563 optimization during design can be greatly reduced. Surrogates could be used  
564 while considering new constraints to allow for more rapid design, and then finally  
565 rebuilt once constraints are more firmly understood. While this was not the fo-  
566 cus of this competition, it was encouraging to see a surrogate model achieve  
567 such promising results.

568 This competition also encouraged the use of intelligent stop criteria by allow-  
569 ing competitors to develop a strategy to best allocate their evaluation over the  
570 five scenarios. The stop criterion of the optimization is still an open question

571 for evolutionary algorithms and is a difficult one to address: even if evolution-  
572 ary algorithms have been proven to converge to the optimal solution [33], it is  
573 impossible to determine when and even if the current best solution is a local  
574 optimum or the global one. This is due to the size of search space explored  
575 in this kind of problem. However, transformations on the search space can re-  
576 duce its complexity, and the convergence of most algorithms here suggests that  
577 simpler search space created by optimizing geometric parameters allows for a  
578 more natural stop condition. Furthermore, we imagine the integration of this  
579 type of optimization into wind layout software will be part of an iterative design  
580 process, as numerous factors, including human design, come into play during  
581 wind farm design. The optimization process could be run for a desired num-  
582 ber of steps or amount of computational time before being further reviewed or  
583 modified, matching the needs of human designers and mitigating the issue of a  
584 stop criterion.

#### 585 **Acknowledgments**

586 D. Wilson is supported by ANR-11-LABX-0040-CIMI, within programme  
587 ANR-11-IDEX-0002-02. C. Segura acknowledges the financial support from  
588 CONACyT through the “Cienca Básica” project no. 285599. The work of A.  
589 Kheiri and E. Keedwell was funded by EPSRC grant no. EP/K000519/1.



590 **References**

- 591 [1] Andrew Kusiak and Zhe Song. Design of wind farm layout for maximum  
592 wind energy capture. *Renewable Energy*, 35(3):685–694, 2010.
- 593 [2] G Mosetti, Carlo Poloni, and B Diviacco. Optimization of wind turbine  
594 positioning in large windfarms by means of a genetic algorithm. *Journal of*  
595 *Wind Engineering and Industrial Aerodynamics*, 51(1):105–116, 1994.
- 596 [3] SA Grady, MY Hussaini, and Makola M Abdullah. Placement of wind  
597 turbines using genetic algorithms. *Renewable Energy*, 30(2):259–270, 2005.
- 598 [4] Hou-Sheng Huang. Distributed genetic algorithm for optimization of wind  
599 farm annual profits. In *Intelligent Systems Applications to Power Systems,*  
600 *2007. ISAP 2007. International Conference on*, pages 1–6. IEEE, 2007.
- 601 [5] Chunqiu Wan, Jun Wang, Geng Yang, Xiaolan Li, and Xing Zhang. Opti-  
602 mal micro-siting of wind turbines by genetic algorithms based on improved  
603 wind and turbine models. In *Decision and Control, 2009 held jointly with*  
604 *the 2009 28th Chinese Control Conference. CDC/CCC 2009. Proceedings*  
605 *of the 48th IEEE Conference on*, pages 5092–5096. IEEE, 2009.
- 606 [6] Alireza Emami and Pirooz Noghreh. New approach on optimization in  
607 placement of wind turbines within wind farm by genetic algorithms. *Re-*  
608 *newable Energy*, 35(7):1559–1564, 2010.
- 609 [7] Sedat Şişbot, Özgü Turgut, Murat Tunç, and Ünal Çamdalı. Optimal  
610 positioning of wind turbines on gökçeada using multi-objective genetic al-  
611 gorithm. *Wind Energy*, 13(4):297–306, 2010.
- 612 [8] Chang Xu, Yan Yan, De You Liu, Yuan Zheng, and Chen Qi Li. Opti-  
613 mization of wind farm micro sitting based on genetic algorithm. *Advanced*  
614 *Materials Research*, 347:3545–3550, 2012.
- 615 [9] Chunqiu Wan, Jun Wang, Geng Yang, and Xing Zhang. Optimal micro-  
616 siting of wind farms by particle swarm optimization. In *Advances in swarm*  
617 *intelligence*, pages 198–205. Springer, 2010.
- 618 [10] Souma Chowdhury, Jie Zhang, Achille Messac, and Luciano Castillo. Un-  
619 restricted wind farm layout optimization (uwflo): Investigating key factors  
620 influencing the maximum power generation. *Renewable Energy*, 38(1):16–  
621 30, 2012.
- 622 [11] Kalyan Veeramachaneni, Markus Wagner, U-M O’Reilly, and Frank Neu-  
623 mann. Optimizing energy output and layout costs for large wind farms  
624 using particle swarm optimization. In *Evolutionary Computation (CEC),*  
625 *2012 IEEE Congress on*, pages 1–7. IEEE, 2012.
- 626 [12] Markus Wagner, Jareth Day, and Frank Neumann. A fast and effective local  
627 search algorithm for optimizing the placement of wind turbines. *Renewable*  
628 *Energy*, 51(0):64 – 70, 2013.

- 629 [13] Markus Wagner, Kalyan Veeramachaneni, Frank Neumann, and Una-May  
630 O'Reilly. Optimizing the layout of 1000 wind turbines. *European Wind*  
631 *Energy Association Annual Event*, pages 205–209, 2011.
- 632 [14] Dennis Wilson, Sylvain Cussat-Blanc, Kalyan Veeramachaneni, Una-May  
633 O'Reilly, and Hervé Luga. A continuous developmental model for wind  
634 farm layout optimization. In *Proceedings of the 2014 Annual Conference*  
635 *on Genetic and Evolutionary Computation*, pages 745–752. ACM, 2014.
- 636 [15] Salman A Khan and Shafiqur Rehman. Iterative non-deterministic algo-  
637 rithms in on-shore wind farm design: A brief survey. *Renewable and Sus-*  
638 *tainable Energy Reviews*, 19:370–384, 2013.
- 639 [16] Michele Samorani. The wind farm layout optimization problem. In *Hand-*  
640 *book of wind power systems*, pages 21–38. Springer, 2013.
- 641 [17] Yaochu Jin. Surrogate-assisted evolutionary computation: Recent advances  
642 and future challenges. *Swarm and Evolutionary Computation*, 1(2):61 – 70,  
643 2011.
- 644 [18] Alexander E.I. Brownlee, John R. Woodward, and Jerry Swan. Metaheuristic  
645 design pattern: Surrogate fitness functions. In *Proceedings of the Com-*  
646 *panion Publication of the 2015 Annual Conference on Genetic and Evo-*  
647 *lutionary Computation*, GECCO Companion '15, pages 1261–1264, New  
648 York, NY, USA, 2015. ACM.
- 649 [19] K. Price, R.M. Storn, and J. Lampinen. *Differential Evolution: A Prac-*  
650 *tical Approach to Global Optimization*. Natural Computing Series. U.S.  
651 Government Printing Office, 2005.
- 652 [20] A.E. Eiben and J.E. Smith. *Introduction to Evolutionary Computing*. Nat-  
653 ural Computing Series. Springer, 2003.
- 654 [21] N. Hansen, S.D. Müller, and P. Koumoutsakos. Reducing the time complex-  
655 ity of the derandomized evolution strategy with covariance matrix adapta-  
656 tion (CMA-ES). *Evolutionary Computation*, 11(1):1–18, 2003.
- 657 [22] S. Finck, N. Hansen, R. Ros, and A. Auger. Real-parameter black-box  
658 optimization benchmarking 2010: Experimental setup. Technical Report  
659 2009/21, Research Center PPE, 2010.
- 660 [23] A. Auger, S. Finck, N. Hansen, and R. Ros. BBOB 2010: Comparison  
661 Tables of All Algorithms on All Noiseless Functions. Technical Report  
662 RR-7215, INRIA, 2010.
- 663 [24] Ilya Loshchilov, Marc Schoenauer, and Michèle Sebag. Bi-population CMA-  
664 ES algorithms with surrogate models and line searches. In *Genetic and*  
665 *Evolutionary Computation Conference*, pages 1177–1184. ACM, 2013.

- 666 [25] Salvador García, Daniel Molina, Manuel Lozano, and Francisco Herrera.  
667 A study on the use of non-parametric tests for analyzing the evolutionary  
668 algorithms' behaviour: a case study on the CEC'2005 Special Session on  
669 Real Parameter Optimization. *Journal of Heuristics*, 15:617–644, 2009.
- 670 [26] Ilya Loshchilov. CMA-ES with restarts for solving CEC 2013 benchmark  
671 problems. In *Evolutionary Computation (CEC), 2013 IEEE Congress on*,  
672 pages 369–376. IEEE, 2013.
- 673 [27] Nikolaus Hansen and Raymond Ros. Benchmarking a weighted negative  
674 covariance matrix update on the BBOB-2010 noiseless testbed. In *Genetic  
675 and Evolutionary Computation Conference*, pages 1673–1680. ACM, 2010.
- 676 [28] Graheme A. Jastrebski and Dirk V. Arnold. Improving Evolution Strategies  
677 through Active Covariance Matrix Adaptation. In *IEEE Congress on  
678 Evolutionary Computation*, pages 2814–2821, 2006.
- 679 [29] E. K. Burke, M. Gendreau, M. Hyde, G. Kendall, G. Ochoa, E. Özcan, and  
680 R. Qu. Hyper-heuristics: a survey of the state of the art. *Journal of the  
681 Operational Research Society*, 64(12):1695–1724, 2013.
- 682 [30] Ahmed Kheiri and Ed Keedwell. A hidden markov model approach to the  
683 problem of heuristic selection in hyper-heuristics with a case study in high  
684 school timetabling problems. *Evolutionary Computation*, 25(3):473–501,  
685 2017.
- 686 [31] Ahmed Kheiri and Ed Keedwell. A sequence-based selection hyper-heuristic  
687 utilising a hidden Markov model. In *Proceedings of the 2015 on Genetic  
688 and Evolutionary Computation Conference, GECCO '15*, pages 417–424,  
689 New York, NY, USA, 2015. ACM.
- 690 [32] Ahmed Kheiri, Edward Keedwell, Michael J. Gibson, and Dragan Savic. Se-  
691 quence analysis-based hyper-heuristics for water distribution network opti-  
692 misation. *Procedia Engineering*, 119:1269–1277, 2015. Computing and  
693 Control for the Water Industry (CCWI2015) Sharing the best practice in  
694 water management.
- 695 [33] Agoston E Eiben, Emile HL Aarts, and Kees M Van Hee. Global con-  
696 vergence of genetic algorithms: A markov chain analysis. In *International  
697 Conference on Parallel Problem Solving from Nature*, pages 3–12. Springer,  
698 1990.

## Research highlights:

- Optimizing wind turbines positions.
- Use of evolutionary algorithm.
- Report on the 2015 wind farm layout optimization competition.
- Compare new algorithms with state-of-the-art approaches.

ACCEPTED MANUSCRIPT